Title

Phenotypic and Genotypic Characterization of Daptomycin-Resistant Methicillin-Resistant Staphylococcus aureus Strains: Relative Roles of mprF and dlt Operons

Journal

PLOS ONE, 9(9)

ISSN

1932-6203

Authors

Mishra, Nagendra N
Bayer, Arnold S
Weidenmaier, Christopher
et al.

Publication Date

2014

DOI

10.1371/journal.pone.0107426

OPEN ACCESS Freely available online

PLOS ONE

Phenotypic and Genotypic Characterization of Daptomycin-Resistant Methicillin-Resistant *Staphylococcus aureus* Strains: Relative Roles of *mprF* and *dlt* Operons

Nagendra N. Mishra[1,2☯], Arnold S. Bayer[1,2☯], Christopher Weidenmaier[3,4], Timo Grau[3], Stefanie Wanner[3], Stefania Stefani[5], Viviana Cafiso[5], Taschia Bertuccio[5], Michael R. Yeaman[1,2,6], Cynthia C. Nast[2,7], Soo-Jin Yang[1,2]*

1 Division of Infectious Diseases, Los Angeles Biomedical Research Institute at Harbor-UCLA Medical Center, Torrance, California, United States of America, **2** The David Geffen School of Medicine at UCLA, Los Angeles, California, United States of America, **3** Interfaculty Institute of Microbiology and Infection Medicine, University of Tübingen, Tübingen, Germany, **4** German Center for Infection Research (DZIF), Tübingen, Germany, **5** Department of Biomedical Sciences-Microbiology, University of Catania, Catania, Italy, **6** Division of Molecular Medicine, Harbor-UCLA Medical Center, Torrance, California, United States of America, **7** Cedars-Sinai Medical Center, Los Angeles, California, United States of America

Abstract

Development of *in vivo* daptomycin resistance (DAP-R) among *Staphylococcus aureus* clinical isolates, in association with clinical treatment failures, has become a major therapeutic problem. This issue is especially relevant to methicillin-resistant *S. aureus* (MRSA) strains in the context of invasive endovascular infections. In the current study, we used three well-characterized and clinically-derived DAP-susceptible (DAP-S) vs. resistant (DAP-R) MRSA strain-pairs to elucidate potential genotypic mechanisms of the DAP-R phenotype. In comparison to the DAP-S parental strains, DAP-R isolates demonstrated (**i**) altered expression of two key determinants of net positive surface charge, either during exponential or stationary growth phases (i.e., dysregulation of *dltA and mprF*), (**ii**) a significant increase in the D-alanylated wall teichoic acid (WTA) content in DAP-R strains, reflecting DltA gain-in-function; (**iii**) heightened elaboration of lysinylated-phosphatidylglyderol (L-PG) in DAP-R strains, reflecting MprF gain-in-function; (**iv**) increased cell membrane (CM) fluidity, and (**v**) significantly reduced susceptibility to prototypic cationic host defense peptides of platelet and leukocyte origins. In the tested DAP-R strains, genes conferring positive surface charge were dysregulated, and their functionality altered. However, there were no correlations between relative surface positive charge or cell wall thickness and the observed DAP-R phenotype. Thus, charge repulsion mechanisms via altered surface charge may not be sufficient to explain the DAP-R outcome. Instead, changes in the compositional or biophysical order of the DAP CM target of such DAP-R strains (i.e., increased fluidity) may be essential to this phenotype. Taken together, DAP-R in *S. aureus* appears to involve multi-factorial and strain-specific adaptive mechanisms.

Citation: Mishra NN, Bayer AS, Weidenmaier C, Grau T, Wanner S, et al. (2014) Phenotypic and Genotypic Characterization of Daptomycin-Resistant Methicillin-Resistant *Staphylococcus aureus* Strains: Relative Roles of *mprF* and *dlt* Operons. PLoS ONE 9(9): e107426. doi:10.1371/journal.pone.0107426

Editor: Franklin D. Lowy, Columbia University, College of Physicians and Surgeons, United States of America

Received June 4, 2014; **Accepted** August 9, 2014; **Published** September 16, 2014

Data Availability: The authors confirm that all data underlying the findings are fully available without restriction. All relevant data are within the paper and its Supporting Information files.

Funding: This research was supported in-part by grants from National Institutes of Health (AI-39108-15 to A.S.B and AI-111611 to MRY), the U.S. Department of Defense (W81XWH-12-2-0101 to MRY), the American Heart Association (12BGIA11780035 to SJY), and the German Research Foundation (TR-SFB34 and SFB766 to CW). The funders had no role in study design, data collection and analysis, decision to publish, or preparation of the manuscript.

Competing Interests: The authors have declared that no competing interests exist.

* Email: sjyang@ucla.edu

☯ These authors contributed equally to this work.

Introduction

Daptomycin (**DAP**) is a calcium-dependent lipopeptide antibiotic with potent bactericidal effects against most Gram-positive pathogens [1,2]. Since its release for use in 2003 for skin and soft tissue infections, followed by approval for *Staphylococcus aureus* bacteremia and right-sided endocarditis in 2006, DAP has become a key antibiotic for invasive staphylococcal infections. This is especially relevant to methicillin-resistant *S. aureus* (**MRSA**) infections in the era of rising vancomycin MICs associated with clinical treatment failures [3–5], as well as vancomycin (VAN)-intermediate *S. aureus* (VISA)-related infections [2,5,6]. Recently, there have been an alarming number of reports of both *S. aureus* and enterococcal DAP-resistant (**DAP-R**) strains emerging during DAP treatment failures [7–12]. The mechanisms by which such organisms develop resistance to the microbicidal effects of DAP are likely multi-modal and organism-dependent [9,13–18]. Thus, integrative genotypic and phenotypic profiles among DAP-R *S. aureus* strains differ substantially from those defined among DAP-R enterococci [9,10,13,14,16–18]. Moreover, although a principle

mechanism of DAP action appears to be perturbation of the bacterial cell membrane (**CM**), key impacts upon cell wall (**CW**) turnover processes seem to play a cardinal role in this regard [19–21]. Since DAP unambiguously requires calcium complexing to execute its CM-targeting and subsequent bactericidal effects, this agent acts similarly to cationic antimicrobial peptides involved in innate host defenses (e.g., from PMNs and platelets [22,23]). The range of potential phenotypic adaptations that may be associated with staphylococcal DAP-R include: **i**) increased positive surface charge ('charge-repulsion hypothesis') [9,17,18,24]; **ii**) altered CM fatty acid composition resulting in altered CM fluidity [14,25,26] ('membrane order hypothesis'); **iii**) increased CM carotenoid pigment content yielding very rigid CMs [27]; **iv**) a combination of factors; for example, enhanced CM content of positively-charged phospholipids, as well as increased D-alanylation of CW teichoic acid, resulting in reduced affinity of DAP to the CM target [28]; and **v**) augmented synthesis of CW teichoic acid, creating a thickened CW phenotype and a putative mechanical barrier to DAP penetration to reach its CM target [28,29].

The above phenotypic correlates of DAP-R in *S. aureus* point to specific genes as potentially involved in this resistance process. In this regard, the *mprF* operon (involved in lysinylation of CM phosphatidylglycerol [PG] to synthesize lysyl-PG [L-PG], as well as to translocate this latter positively-charged species to the outer CM) and the *dlt* operon (responsible for the D-alanylation of CW teichoic acid) have received particular attention [17,24,28–33]. However, studies have varied widely in ascribing causality to these two loci in DAP-R *S. aureus* strains, since a broad range of genotypic correlates with the DAP-R phenotype have emerged, including: **i**) acquisition of gain-in-function single nucleotide polymorphisms (**SNPs**) in the *mprF* ORF [9,11,24,25,34]; **ii**) over-expression of *dlt* genes [17]; and **iii**) dysregulation of both *mprF* and *dlt* expression profiles [17,24,29]. Recently, Cafiso et al [31] studied three clinical MRSA strain-sets in which DAP-R evolved during treatment, and were able to pinpoint *dltA* overexpression (especially in strains acquiring a concomitant SNP in *mprF*) as potentially causal in the DAP-R phenotype. This intriguing investigation was, however, somewhat limited, in that within the DAP-S and DAP-R strain-sets: **i**) there was no growth phase-dependent gene expression profiling performed; **ii**) there were no phenotypic correlates of *dlt* and *mprF* over-expression studied, especially surface charge measurements; **iii**) specific phenotypic readouts of *dlt* and *mprF* over-expression were not quantified (i.e., CW D-alanylation and CM L-PG synthesis and/or translocation, respectively [25,28,32]); **iv**) other parameters of CM physiology previously associated with DAP-R (e.g., CM fluidity and fatty acid contents) were not queried [9,27,35]; and **v**) assessment of DAP-R isolates for *in vitro* 'cross-resistance' with several prototypical host defense cationic peptides (**HDPs**) involved in staphylococcal pathogenesis was not performed [9,18,25,35]. The latter cross-resistance phenomenon has been well-chronicled for other DAP-R *S. aureus* strains [25]. The current study, employing the same previously published DAP-S/DAP-R strain-pairs [31], was designed to address these limitations, and to further characterize potential mechanisms of DAP-R in these strains.

Methods and Materials

Bacterial strains

The three clinically-derived DAP-S/DAP-R MRSA strain-pairs used in the current study (**Table 1**) have been described in detail before [31]. Briefly, the epidemiologically unrelated stran-pairs were isolated from different patients, were from different clinical infection types (skin and soft tissue; bacteremia), and were from three different Italian hospitals. All three patients had received and failed therapy with the glycopeptides antibiotic, teicoplanin, and were subsequently treated with DAP [31]. Each strain-pair included an initial pre-DAP therapy DAP-S MRSA strain and an isogenic DAP-R isolate obtained during DAP therapy. Isogenicity of each strain-pair was confirmed by identical outcomes of several discriminative genotypic assays within each DAP-S and DAP-R strain-pair, including: pulse field gel electrophoresis typing (PFGE), *agr* typing, multi-locus sequence typing and staphylococcal casette chromosome (SCC*mec*) typing. The three strain-pairs were previously characterized for mutations in the *mprF* genes. Two of the three DAP-R variants within each strain-pair exhibited a non-synonomous SNP in the *mprF* ORF (**Table 1**), while the third strain-set did not. Of note, these two SNPs occurred in previously described "hotspots" within the *mprF* locus associated with MprF gains-in-function and the DAP-R phenotype [9,32,34]. The above genotypic data for these three strain-pairs have been previously published [31].

MIC testing

Oxacillin, vancomycin and DAP MICs were performed according to CLSI guidelines [36]. These data have been previously reported (**Table 1**) [31].

Surface charge

The cytochrome *c* binding assay was performed as a surrogate measure of the relative net positive surface charge of the strain-pairs as described previously [17,18,37]. Briefly, cells were grown overnight in TSB media, washed with 20 mM MOPS buffer (pH 7.0) three times and resuspended in the same buffer at $OD_{578} = 1.0$. Cells were incubated with 0.5 mg/ml cytochrome *c* for 10 minutes and the amount of cytochrome *c* remaining in the supernatant was determined spectrophotometrically at OD_{530} nm. The more unbound cytochrome *c* that was detected in the supernatant, the more net positively charged the bacterial surface. Data were converted and expressed as mean (± SD) amount of bound cytochrome *c*. At least three independent runs were performed on separate days.

Wall teichoic acid (WTA) isolation and purification

S. aureus CW and WTA were specifically isolated as described in detail before [39,40]. In brief, bacteria were grown overnight in B-Medium (1% peptone, 0.5% yeast extract, 0.1% glucose, 0.5% NaCl and 0.1% K_2HPO_4) containing 0.25% (wt/vol) glucose, washed twice in sodium acetate buffer (20 mM, pH 4.7) and disrupted in the same buffer with glass beads for 1 h on ice in a cell disruptor (Euler). Protein-free CW was isolated, and WTA was released by treatment with 5% trichloroacetic acid in sodium acetate buffer for 4 h at 60°C. The CWs were removed by centrifugation and WTA was quantified by determining its inorganic phosphate (Pi) content as described before [40]. The isolation was performed in triplicate for each strain, and assayed in triplicate for their respective Pi content.

Quantification of D-alanylated WTA content

The D-alanylation of the WTA polymers was assayed and quantified as described before [41]. In brief, D-alanine esters were hydrolyzed by a mild alkaline hydrolysis carried out at 37°C for 1 h in 0.1 M NaOH. The supernatant was neutralized, dried under vacuum, and used for pre-column derivatization with Marfey's reagent (1-fluoro-2, 4-dinitrophenyl-5-L-alanine amide; Sigma). Amino acid derivates (detection at 340 nm) were then

Table 1. Bacterial strains examined in the current studies. *

Strain	ST type	SCC*mec*	PFGE	*agr* type	DAP MICs	VANC MICs	*mprF* SNPs
1A	398	IVa	ApaI/SmaI	I	≤0.25	1	-
1C	398	IVa	ApaI/SmaI	I	4	2	S295L
2B	5	II	USA100	II	0.5	1	-
2C	5	II	USA100	II	2	2	T345I
3A	22	IV	G1	I	0.5	1	-
3B	22	IV	G1	I	4	2	-

*These data have been previously published [31]; DAP = daptomycin; VAN = vancomycin; SNPs = single nucleotide polymorphisms.
doi:10.1371/journal.pone.0107426.t001

separated as described before and analyzed with the ChemStation software. Data were expressed as percent of WTA (± SD) that was D-alanylated. A minimum of three independent runs was performed.

Cell wall (CW) thickness

The CW thickness of study strains were measured by transmission electron microscopy (TEM; [25,26]). The mean CW thickness (nm ± SD) of 100 cells was determined for the strains at a constant magnification of 190,000× (JEOL, Model# 100CX, Tokyo, Japan) using digital image capture and morphometric measurement (Advanced Microscopy Techniques v54, Danvers, MA).

Host defense peptides (HDPs)

Thrombin-induced platelet microbicidal proteins (tPMPs) were obtained from thrombin-stimulated rabbit platelets as previously described [43]. This preparation contains several tPMPs, but predominantly tPMP-1. The bioequivalency (activity in μg/ml) of the tPMP preparation was determined as detailed before, using a *Bacillus subtilis* bioassay [9]. Purified human neutrophil defensin-1 (hNP-1) and LL-37 (prevalent in neutrophils and skin epithelium [22,44,45]) were purchased from Peptides International (Louisville, KY). RP-1 (a synthetic congener of the microbicidal domain of the platelet factor-4 family of kinocidins) was synthesized as previously detailed [46].

Susceptibilities to HDPs

For tPMPs and RP-1, a microtiter bactericidal assay was carried out in minimal liquid nutrient medium (Eagles minimal essential media [MEM]) in appropriate buffers [25]; the hNP-1 and LL-37 killing assays were performed in 1% BHI +10 mM potassium phosphate buffer (PPB). A final bacterial inoculum of 10^3 stationary phase CFU was employed. The peptide concentrations used in the 2 h killing assays were: 1.5 or 2.0 μg/ml bioactivity equivalent for tPMPs; 5 or 10 for hNP-1; and 0.5 and 1 μg/ml for RP-1 and LL-37. After extensive pilot studies, these peptide concentrations were selected based on: (**i**) sub-lethality, with < 50% reductions in counts of the parental DAP-susceptible (DAP-S) strain; and (**ii**) encompassing peptide concentrations used in prior investigations of HDP:*S. aureus* interactions [25]. After 2 h peptide exposure, samples were obtained and processed for quantitative culture to evaluate the extent of killing by each HDP condition. Final data were expressed as mean (± SD) percent survival rate. Since there is no *bona fide* "resistance" breakpoint for HDPs, the mean percent survival (± SD) was statistically evaluated for potential correlates of HDP and DAP susceptibility profiles. Data included a minimum of three experiments performed on separate days.

CM phospholipid (PL) and amino-PL translocation (asymmetry)

To investigate potential correlates between *mprF* polymorphisms and CM features, PLs were extracted from study strains under specific test conditions as described [26]. The major CM PLs of *S. aureus* (PG; L-PG and cardiolipin [CL]) were separated by two-dimensional thin-layer chromatography (2-D TLC) using Silica 60 F254 HPTLC plates (Merck). Fluorescamine labeling (a fluorophore which binds only to positively charged PLs, such as L-PG, and which does not penetrate the outer CM leaflet), combined with ninhydrin staining localization, was used within the 2-D TLC plate assay to assess the translocation of L-PG between the inner-to-outer CM bilayer [13,17,26]. First-dimension chloroform-

Table 2. *In vitro* susceptibility to killing by cationic host defense peptides and the congener, RP-1.

Strain	% survival (mean ± SD) after 2-h exposure to:							
	tPMPs (2 μg/ml)	tPMPs (1 μg/ml)	LL-37 (1 μg/ml)	LL-37 (0.5 μg/ml)	hNP-1 (20 μg/ml)	hNP-1 (10 μg/ml)	RP-1 (1 μg/ml)	RP-1 (0.5 μg/ml)
1A	2.5±2.0	4.7±3.8	0.5±0.9	11.7±6.0	46.3±18.9	72.6±22.2	4.3±3.2	15.9±9.6
1C	18.0±13.5**	38.1±15.3*	36.1±17.6**	59.0±19.0**	68.2±19.2*	79.2±19.6	22.3±12.5**	52.7±14.7**
2A	4.1±3.2	19.4±9.9	0.5±0.7	13.1±11.8	44.20±30.4	60.8±26.1	1.4±1.2	11.3±5.4
2C	83.0±8.4**	90.8±11.4**	22.4±12.6**	65.9±26.1**	66.0±18.0	92.1±17.5*	4.7±5.0	26.1±15.1*
3A	7.4±5.8	25.9±11.9	1.8±2.5	62.0±20.8	35.6±26.1	60.3±24.2	1.0±1.5	17.3±8.5
3B	80.4±13.5**	86.7±12.1**	49.9±19.9**	99.6±10.4**	88.7±15.2**	91.1±8.6**	10.9±9.6*	34.5±12.2*

*$P<0.05$;
**$P<0.01$ vs the DAP-S parental strains.
doi:10.1371/journal.pone.0107426.t002

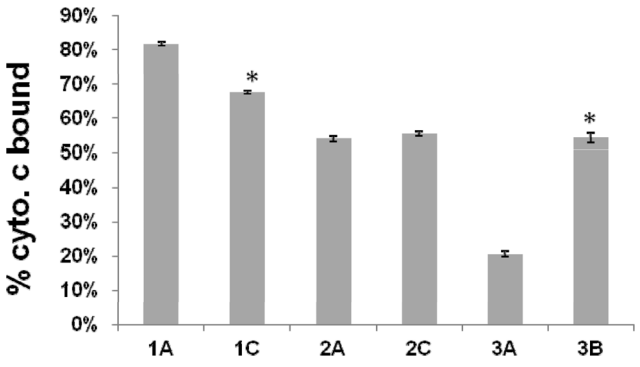

Figure 1. Relative positive surface charge by cytochrome *c* binding. The graph shows percent of cytochrome *c* bound after 10 min of incubation with *S. aureus* cells at room temperature. Data represent the means and standard deviations from three independent experiments. *$P<0.01$ vs DAP-S parental strains.
doi:10.1371/journal.pone.0107426.g001

methanol–25% ammonium hydroxide (65:25:6, by volume) in the vertical orientation and second-dimension chloroform:water:-methanol:glacial acetic acid:acetone (45:4:8:9:16, by volume) in the horizontal orientation were used for the separation of the PLs for further quantitation by phosphate estimation. PL identity was confirmed using known PL standards. For quantitative analysis, resulting isolated PLs (identified by iodine staining) were digested at 180°C for 3 h with 0.3 ml 70% perchloric acid and the oxidized derivatives quantified spectrophotometrically at OD_{660}.

CM fatty acid composition

Given the impact of fatty acid composition on CM adaptability to stress, the comparative fatty acid profiles of the DAP-S/DAP-R strain-pairs were determined. Approximately 20 mg of bacterial cells were harvested from late log phase growth preparations, and then saponified, methylated, and fatty acid esters extracted into hexane as described previously [17,26]. The resulting methyl ester mixtures were separated by an Agilent 5890 dual-tower gas chromatograph. Fatty acids were identified and quantified by a microbial identification system (Sherlock 4.5; courtesy of Microbial ID Inc., Newark, DE) [17,26].

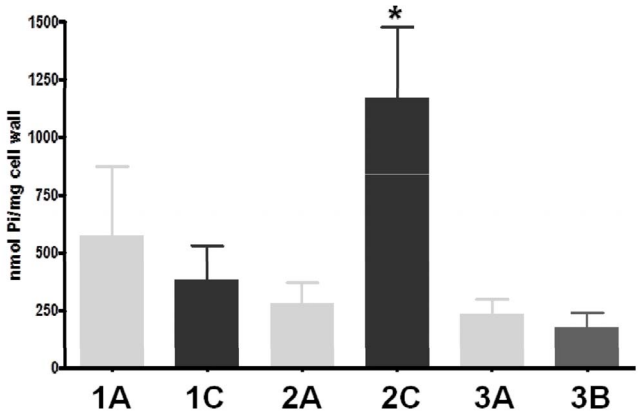

Figure 2. Cell wall teichoic acid (WTA) contents of the strain sets. Dry mass of cell wall was quantified as [g dry weight/g wet weight]. The amount of WTA was determined by a colorimetric assay and expressed as [nmol Pi/mg cell wall; n = 5]. Statistical analysis was performed by Student's t-test. *$P<0.05$ vs DAP-S parental strain.
doi:10.1371/journal.pone.0107426.g002

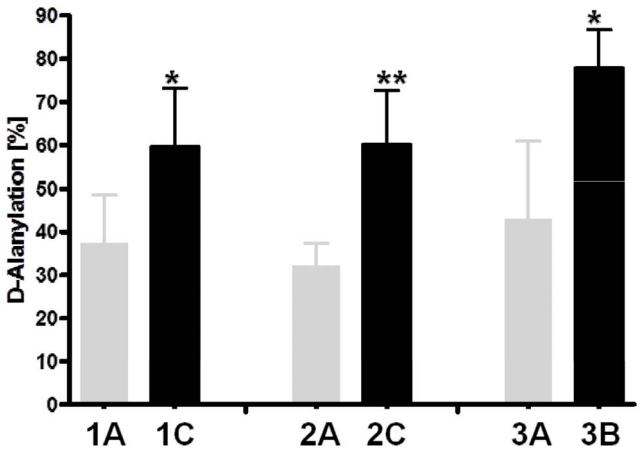

Figure 3. WTA D-alanylation in the DAP-S/DAP-R strain pairs. The rate of D-alanylation of WTA repeating units was determined by HPLC (n = 3). Statistical analysis was performed by Student's t-test. *$P<$ 0.05; **$P<0.01$ vs DAP-S parental strains.
doi:10.1371/journal.pone.0107426.g003

CM fluidity

CM fluidity was determined by fluorescence polarization spectrofluorometry as detailed previously [9,25,26] using the fluorescent probe 1,6-diphenyl-1,3,5-hexatriene (DPH). An inverse relationship exists between polarization indices and the degree of CM order (i.e., lower polarization indices [PI value] denotes a greater CM fluidity) [9,25,26]. To address day-to-day biological variability inherent to CM dynamics, these assays were performed a minimum of six times for each strain on separate days.

DNA isolation and targeted *mprF, dltA, and dltB* sequencing

Genomic DNA was isolated from *S. aureus* using the method of Dyer and Iandolo [47]. PCR amplification of the *mprF* ORF was performed as we have previously described, using the primers, *mprF*-F-bam (5′-CCCGGATCCAATTAGAATTGATGTGA-AAAAATG-3′) and *mprF*-R-sph (5′-CCCGCATGCAGCGCTT-CAGGCATAACTGT-3′) [24].

PCR amplification of the *dltA* and *dltB* ORFs were performed as we have described previously with primer pairs dltA-ORF-F (5′-CAGTGGCGACACACACAATA-3′) and dltA-ORF-R (5′-GACTGGTAATAATGCAATTAAAGCAA-3′), dltB-ORF-F (5′-TGGAACAATTGCCATTGACTT-3′) and dltB-ORF-R (5′-TCCAACTGTTTGGAAAGA ATCA-3′), respectively [17]. DNA sequencing of the *mprF and dlt genes* was kindly performed at City of Hope, Duarte, CA.

RNA isolation and qRT-PCR analysis for *mprF* and *dltA* transcription

For RNA isolation, fresh overnight cultures of *S. aureus* strains were used to inoculate NZY broth to an optical density at 600 nm (OD_{600}) of 0.1. Cells were harvested during both exponential growth (2.5 h; OD = 0.5) and stationary phase (12 h). Total RNA was isolated from the cell pellets by using the RNeasy kit (Qiagen, Valencia, CA) and the FASTPREP FP120 instrument (BIO 101, Vista, CA), according to the manufacturer's recommended protocols.

Quantitative real time PCR assay was carried out as detailed previously [29,48]. Briefly, 1 μg of DNase-treated RNA was reverse transcribed using the SuperScript III first-strand synthesis kit (Invitrogen) according to the manufacturer's protocols. Quantification of cDNA levels was performed following the instructions of the Power SYBR green master mix kit (Applied Biosystems) on an ABI PRISM 7000 sequence detection system (Applied Biosystems) or on a LightCycler using the Quanti Fast SYBR green real-time (RT)-PCR kit (Qiagen). The *mprF, dltA,* and *gyrB* genes were detected using specific primers and computational methods as described before [29,48].

Results

HDP susceptibility profiles

As anticipated, the peptides exerted distinct efficacies against the study strains (**Table 2**). RP-1 exhibited the greatest anti-staphylococcal activity, including against stain 2C which exhibited high level resistance to other peptides (**Table 2**). There was a general trend for all HDPs tested, showing that the DAP-R isolate in each strain-pair was significantly more resistant to peptide-mediated killing than its DAP-S parental strain. This difference in HDP killing profiles between DAP-S/DAP-R strain-pairs was most dramatic for tPMPs and RP-1 of platelet origin, and LL-37 from leukocytes, while being the least notable for hNP-1 (by far the least active of the peptides against these study strains).

Surface charge (Figure 1)

Outcomes of relative positive surface charge comparisons between DAP-S and DAP-R isolates varied substantially between

Table 3. Comparative fatty acid (FA) compositions of *S. aureus* study strains.

Strains	FA species (% of fatty acid composition ± SD)			
	Iso-BCFA	Anteiso-BCFA	UFAs	SFAs
1A	14.8±0.9	58.6±0.2	8.6±0.9	15.2±0.2
1C	15.9±0.9	57.7±0.2	9.3±0.9	14.5±0.1
2A	17.5±0.7	55.7±2.1	9.0±1.3	15.1±1.3
2C	16.3±0.1	55.2±0.1	9.2±0.1	16.1±0.1
3A	15.5±0.3	53.5±0.3	8.0±0.3	19.8±0.3
3B	13.5±0.3*	62.9±0.8*	7.6±0.5	14.2±0.6*

BCFAs = Branched chain fatty acids; UFAs = unsaturated fatty acids;
SFAs = Saturated fatty acids.
*$P<0.05$ vs. respective parental strain.
doi:10.1371/journal.pone.0107426.t003

Table 4. Comparative cell membrane phospholipid profiles of study strains.

Strains	% of total phospholipids ± SD				
	Inner-LPG	Outer-LPG	Total LPG	PG	CL
1A	11±3.3	2.0±1.0	13±2.8	81±2.8	6±1.4
1C	22±5.5**	5±2.9*	26±7.3**	68±10.2**	6±3.1
2A	9±2.5	2±1.2	11±1.7	84±2.3	5±2.1
2C	19±4.0**	4±4.0	24±6.4**	67±8.9**	9±5.5
3A	19±3.3	3±0.8	22±3.9	69±5.4	9±1.9
3B	13±2.5**	3±1.3	16±3.2*	80±3.6**	4±1.7**

Abbreviations: LPG, lysyl-phosphatydylglycerol; PG, phosphatidylglycerol; CL, cardiolipin.
*$P<0.05$;
**$P<0.01$ vs respective DAP-S parental strains.
doi:10.1371/journal.pone.0107426.t004

strain-pairs. For example, for strain-pair 1, the DAP-R isolate (1C) exhibited a significantly more relative positive surface charge than its parental DAP-S isolate (1A). In contrast, the 3A/3B strain pair showed the exact opposite surface charge relationships; the DAP-S strain 3A bound more cytochrome C than did strain 3C. The 2A/2C strain set had virtually identical surface charge readouts.

Wall teichoic acid (WTA) content (Figure 2)

A significant increase in the amount of WTA in the CW of the DAP-S/DAP-R strain-pair 2A/2C was detected, with the DAP-R strain producing significantly more WTA than the respective DAP-S strain ($P<0.05$). In contrast, in the strain-pairs 1A/1C and 3A/3B, no difference in WTA amount in the CWs of the respective DAP-R strains was detected.

WTA D-alanylation (Figure 3)

In addition to the significant increase in overall WTA content in the DAP-R strain 2C, there was also a substantial difference in the proportion of WTA that was D-alanylated when comparing strain 2C to its isogenic DAP-S strain 2A. Interestingly, the percentage of D-alanine contained within the WTA (nmol D-alanine/nmol Pi) of the DAP-R strains that did not exhibit an increase in WTA content (1C and 3B) was also significantly higher than that observed in their respective DAP-S parental strains (1A and 3A). These latter data speak to a clear-cut gain-in-function of the DltA gene [28,29].

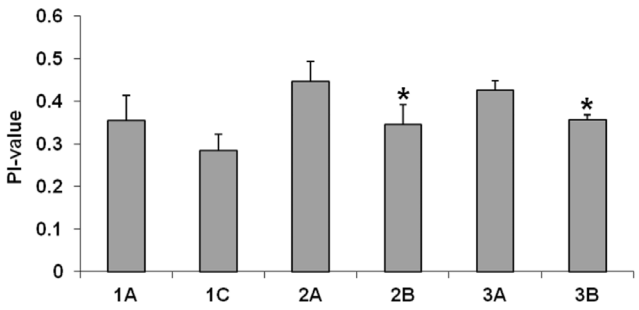

Figure 4. Cell membrane fluidity by fluorescence polarization indices. CM fluidity was determined by using the fluorescent prode 1,6-diphenyl-1,3,5-hexatriene (DPH). These assays were performed a minimum of six times for each strain. Note: Lower polarization indices = higher CM fluidity. *$P<0.05$ vs DAP-S parental strains.
doi:10.1371/journal.pone.0107426.g004

CM fatty acid profiles

Fatty acid compositional data for the three strain-pairs are shown in **Table 3** (a detailed Table enumerating each specific fatty acid species is included as **Table S1**). In two of the three strain-pairs (**1A–1C and 2A–2C**), fatty acid composition exhibited a rather similar overall profile, including proportionality of iso- and ante-iso branched chain fatty acids, unsaturated fatty acids (UFAs), and acyl chain-length profiles. Thus, the increases in CM fluidity observed in the above two DAP-R *S. aureus* strains could not be directly correlated to changes in the proportion of key fatty acids known to impact CM fluidity; i.e, iso- vs anteiso branch chain fatty acids, and saturated vs unsaturated fatty acids). In contrast, in one DAP-R strain (**3B**), fatty acid analyses demonstrated a significant increase in the proportion of anteiso-branch chain species (vs iso-branch chain species) and decrease in saturated fatty acids as compared to its respective parental DAP-S strain (**3A**) ($P<0.05$). In this strain-pair, the total proportions of unsaturated fatty acids were not altered, although an additional fatty acid species (18:2ω6, 9c) was present in DAP-R strain 3B. This increase in anteiso-branch chain species appeared to correspond with a significant reduction in the major iso-branched chain and saturated fatty acid (SFAs) species, respectively, in this DAP-R strain ($P<0.05$). These proportionality perturbations in this latter DAP-R strain provided a potential explanation for the observed increment in CM fluidity in this latter strain (see below).

CM phospholipid (PL) content

Since *mprF* regulates the lysinylation of PG to yield L-PG, as well as its subsequent outer CM translocation, we compared these parameters in the three DAP-S/DAP-R strain pairs. As noted in **Table 4**, in strain pairs 1A/1C and 2A/2C, the DAP-R isolates contained significantly more L-PG than their respective DAP-S parental strains. This outcome was associated with a significant reduction in PG content in both DAP-R isolates. For the third strain-pair (3A/3B), an opposite readout was observed, with the DAP-R strain containing less L-PG than its DAP-S parental strain. Of interest, the outer CM flipping profiles for L-PG did not differ substantially in comparing any DAP-S strain to their respective DAP-R isolates. Thus, the net CM L-PG profile of our study strains reflected the rate of L-PG synthesis, rather than a difference in the extent of CM PL flipping.

CM fluidity (Figure 4)

The polarization indices (PI values) for all three DAP-R isolates were substantially lower than that of their respective DAP-S

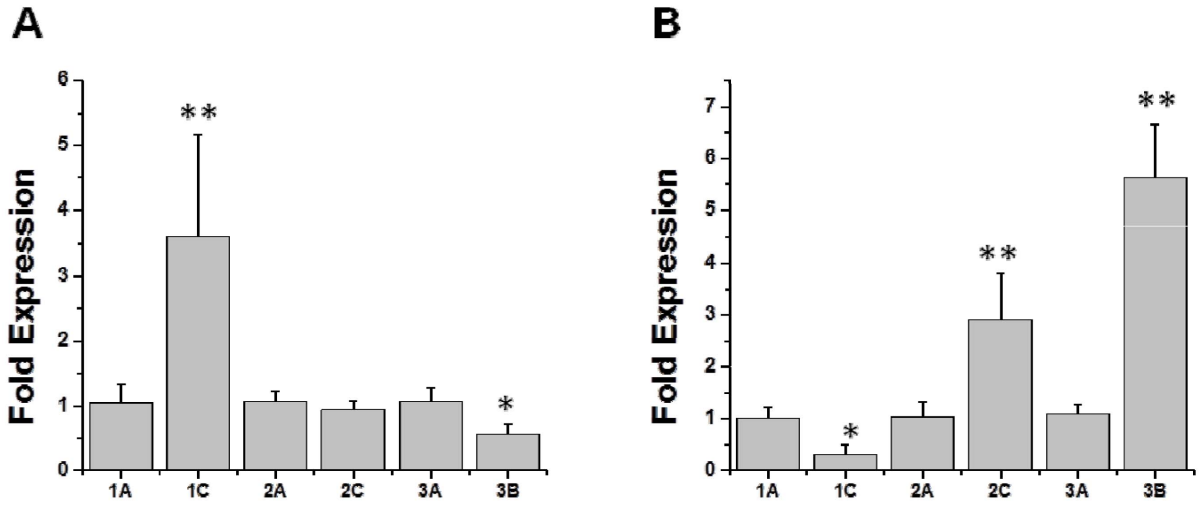

Figure 5. Relative transcription level of *mprF* during exponential (A) and stationary (B) growth phase. RNA samples were isolated from exponential- and stationary-phase cultures of the strains and were subjected to qRT-PCR to detect transcription of *mprF* and *gyrA*. EXPO = exponential growth phase; ST = stationary growth phase; Fold expression = compared to *gyrB* gene, with parental strain fold-expression set at "1". $^{**}P<0.01$ vs DAP-S parental strains.
doi:10.1371/journal.pone.0107426.g005

parental strains, indicating that the CMs of these DAP-R isolates were more fluid than their DAP-S counterparts. These differences reached statistical significance for strain-pairs 2A–2C and 3A–3B.

mprF expression profiles

Figures 5A and 5B demonstrate the relative expression profiles for *mprF* during exponential vs stationary growth phases in these strain-pairs. During exponential growth, the DAP-R strain 1C showed ~4-fold increase in *mprF* expression vs its DAP-S parental strain. Expression profiles for the other two strain pairs did not demonstrate such increases among the DAP-R isolates. In contrast, at stationary growth (when *mprF* expression is generally minimal [24]), the two other DAP-R isolates (2C and 3B) exhibited ~3 and ~6-fold increases, respectively, in *mprF* expression as compared to their DAP-S parental strains. Of note, this stationary phase dysregulation of *mprF* expression in DAP-R strain, 3B, occurred despite the lack of a definable SNP in *mprF* in this isolate.

dltA expression profiles

As shown in **Figures 6A and 6B**, growth phase-dependent *dltA* expression profiles for the DAP-S vs DAP-R strain-pairs showed remarkably similar metrics as for the *mprF* profiles above. Thus, *dltA* expression was increased in DAP-R isolates as compared to their DAP-S parental strain at either exponential or stationary phases of growth.

dltA and *dltB* sequencing

Although a few nucleotide sequence polymorphisms were observed within the *dltA* and *dltB* among the 3 pairs of the strains, only the DAP-R 3B strain revealed one non-synonymous SNP (T-to-C at 763) in the *dltA* gene as compared to its DAP-S

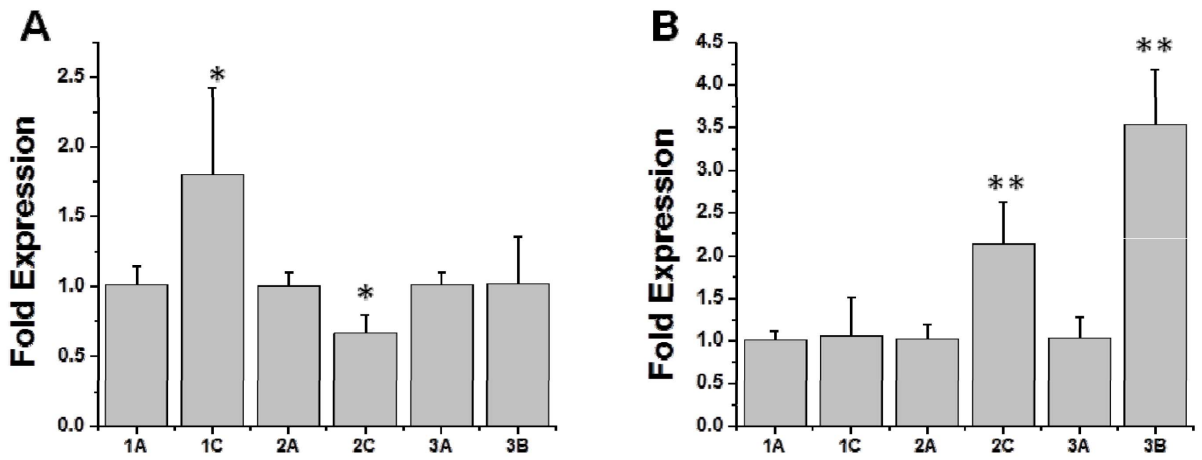

Figure 6. Relative transcription level of *dltA* during exponential (A) and stationary (B) growth phase. RNA samples were isolated from exponential- and stationary-phase cultures of the strains and were subjected to RT-PCR to detect transcription of *dltA* and *gyrA*. EXPO = exponential growth phase; ST = stationary growth phase; Fold expression = compared to *gyrB* gene, with parental strain fold-expression set at "1". $^{*}P<0.05$; $^{**}P<0.01$ vs DAP-S parental strains.
doi:10.1371/journal.pone.0107426.g006

parental strain. This mutation yields a phenylalanine-to-leucine (F255L) amino acid substitution (data not shown). Sequence analyses of *dltB* in the three pairs revealed no differences between the DAP-S and DAP-R pairs.

Discussion

Recently, Cafiso et al [31] have provided further evidence for the potential role of both the CW, and specifically the *dlt* operon in the DAP-R phenotype. These investigators documented the exponential growth-phase enhancement of *dlt* expression in three DAP-R MRSA strains which emerged during DAP therapy, in the presence or absence of *mprF* 'hot spot' SNPs. These authors proposed that *dlt* over-expression is a common pathway of DAP-R. Of note, their data regarding the potential role of *dlt* overexpression and DAP-R mirrors recent findings from our own laboratories [28,29]. However, the investigation of Cafiso et al did not elucidate potential phenotypic or genotypic mechanism(s) by which *dlt* over-expression could be causal in DAP-R.

The current study, utilizing these same DAP-S/DAP-R strain-pairs sought to extend and adjudicate the studies of Cafiso et al [31]. A number of interesting observations emerged from this investigation. *First*, as has been seen previously in selected DAP-R MSSA and MRSA strains [17,28,29,51], *dltA* expression is frequently dysregulated, either by enhanced exponential phase or increased stationary phase transcription profiles. Of interest, *dltA* expression is generally quite minimal at stationary phase in DAP-S *S. aureus* strains [17]. Furthermore, despite these notable differences in *dltA* transcription, only one of the three DAP-R isolates exhibited a non-synonymous SNP in *dltA*. Phenotypically, all three DAP-R strains demonstrated a significant increase in their WTA D-alanylation content, reflecting DltA gains in funtionality. Of interest, concomitant increases in CW thickness were not observed in any of the three DAP-R strains (data not shown).

Second, *mprF* expression profiles were remarkably similar to those of *dltA* above in all three strain-pairs, whether or not 'hot spot' non-synonymous *mprF* SNPs were identified in the DAP-R isolates. The observation that *mprF* transcriptional dysregulation occurred despite the absence of such SNPs supports the notion that regulatory genes outside of *mprF* can affect its expression profile. As expected, phenotypically, in the two DAP-R strains with *mprF* SNPs, enhanced amounts of L-PG synthesis were detected as compared to their respective DAP-S parental isolates. In the remaining DAP-R strain, despite overt *mprF* dysregulation, L-PG synthesis was not increased. This finding is reminiscent of data in selected MSSA DAP-R isolates [9,24].

Third, one prevailing concept that has been put forward to explain the DAP-R phenotype in *S. aureus* has been perturbations in relative cell surface positive charge, creating a "charge repulsion" scenario against calcium complexed-DAP. However, despite the increases in *dltA* transcription, D-alanylation of WTA and L-PG synthesis among the three DAP-R strains, this did not translate into consistent enhancement of surface positive charge in these isolates. These data refute charge repulsion as a principal or comprehensive explanation for the DAP-R phenotype in these strain-pairs.

Fourth, all three DAP-R strains demonstrated substantial increases in their CM fluidity properties as compared to their respective DAP-S parental strains. Altered CM fluidity has been closely linked to resistance to killing by cationic antimicrobial peptides in general [9,19,25]. Such outcomes are presumed to relate to perturbations in the ability of such peptides to interact with and/or insert within target CMs. It is hypothesized that there are biophysical and/or biochemical 'optima' in the CM micro-environments of *S. aureus* strains, making them more or less susceptible to cognate host defense peptides (HDPs) with specific structure-activity signatures. Thus, CMs that exhibit high degrees of rigidity or fluidity are relatively resistant to interactions with specific HDPs that likely rely most upon more intermediate degrees of CM order [25,27]. The global impact of altered fluidity in the current DAP-R vs DAP-S strains is underscored by the *in vitro* "cross-resistance" of the DAP-R strains to cationic HDPs which are structurally distinct from DAP, including prototypical peptides from mammalian platelets and leukocytes. Such cross-resistance between DAP and HDPs has been well-chronicled in recent studies amongst both staphylococci and enterococci [16,25,34,52,53]. The mechanism(s) of enhanced fluidity in the current three DAP-R strains is not entirely clear, although in one DAP-R isolate the ratio of anteiso-branch chain fatty acids (BCFAs) was significantly increased as compared to its DAP-S parental strain. Such iso-to-anteiso-BCFA shifts have been previously associated with increased CM fluidity properties in *Bacillus subtilis* in response to cold shock [54].

Thus, in summary, the ultimate mechanism(s) of DAP-R in *S. aureus* is highly likely to be multi-factorial and strain-specific. Although over-expression and dysregulation of *dltA* transcription may well be identifiable in selected DAP-R *S. aureus* strains and correlated with increased WTA D-alanylation, its subsequent potential phenotypic consequences (i.e., changes in relative surface charge) were not sufficient to entirely explain the DAP-R phenotype in these strains.

Supporting Information

Table S1 Distinct fatty acid (FA) compositions of strain pairs.
(DOC)

Acknowledgments

We thank Kuan-Tsen and Steven N. Ellison for excellent technical assistance with peptide susceptibility testing and *dlt* operon sequencing; and Danya Alvarez for cell membrane fluidity assays.

Author Contributions

Conceived and designed the experiments: NNM ASB CW SJY. Performed the experiments: NNM CW CCN SJY SW. Analyzed the data: NNM ASB MRY CCN SJY. Contributed reagents/materials/analysis tools: SS VC TB TG. Contributed to the writing of the manuscript: NNM ASB CW SS MRY SJY.

References

1. Alborn WE Jr, Allen NE, Preston DA (1991) Daptomycin disrupts membrane potential in growing *Staphylococcus aureus*. Antimicrob Agents Chemother 35: 2282–2287.
2. Schriever CA, Fernandez C, Rodvold KA, Danziger LH (2005) Daptomycin: a novel cyclic lipopeptide antimicrobial. Am J Health Syst Pharm 62: 1145–1158.
3. Boucher HW, Sakoulas G (2007) Antimicrobial resistance: perspectives on daptomycin resistance, with emphasis on resistance in *Staphylococcus aureus*. Clin Infect Dis 45: 601–608.
4. Joson J, Grover C, Downer C, Pujar T, Heidari A (2011) Successful treatment of methicillin-resistant *Staphylococcus aureus* mitral valve endocarditis with sequential linezolid and telavancin monotherapy following daptomycin failure. J Antimicrob Chemother 66: 2186–2188.
5. Marco F, Garcia de la Maria C, Armero Y, Amat E, Soy D, et al. (2008) Daptomycin is effective in treatment of experimental endocarditis due to methicillin-resistant and glycopeptide-intermediate *Staphylococcus aureus*. Antimicrob Agents Chemother 52: 2538–2543.

6. Sakoulas G (2009) Clinical outcomes with daptomycin: a post-marketing, real-world evaluation. Clin Microbiol Infect Suppl: 11–16.
7. Arias CA, Torres HA, Singh KV, Panesso D, Moore J, et al. (2007) Failure of daptomycin monotherapy for endocarditis caused by an *Enterococcus faecium* strain with vancomycin-resistant and vancomycin-susceptible subpopulations and evidence of *in vivo* loss of the *vanA* gene cluster. Clin Infect Dis 45: 1343–1346.
8. Hayden MK, Rezai K, Hayes RA, Lolans K, Quinn JP, et al. (2005) Development of daptomycin resistance *in vivo* in methicillin-resistant *Staphylococcus aureus*. J Clin Microbiol 43: 5285–5287.
9. Jones T, Yeaman MR, Sakoulas G, Yang SJ, Proctor RA, et al. (2008) Failures in clinical treatment of *Staphylococcus aureus* infection with daptomycin are associated with alterations in surface charge, membrane phospholipid asymmetry, and drug binding. Antimicrob Agents Chemother 52: 269–278.
10. Kelesidis T, Tewhey R, Humphries RM (2013) Evolution of high-level daptomycin resistance in *Enterococcus faecium* during daptomycin therapy is associated with limited mutations in the bacterial genome. J Antimicrob Chemother 68: 1926–1928.
11. Murthy MH, Olson ME, Wickert RE, Fey PD, Jalali Z (2008) Daptomycin non-susceptible methicillin-resistant *Staphylococcus aureus* USA 300 isolate. J Medical Microbiol 57: 1036–1038.
12. Skiest DJ (2006) Treatment failure resulting from resistance of *Staphylococcus aureus* to daptomycin. J Clin Microbiol 44: 655–656.
13. Arias CA, Panesso D, McGrath DM, Qin X, Mojica MF, et al. (2011) Genetic basis for in vivo daptomycin resistance in enterococci. N Engl J Med 365: 892–900.
14. Mishra NN, Bayer AS (2013) Correlation of cell membrane lipid profiles with daptomycin resistance in methicillin-resistant *Staphylococcus aureus*. Antimicrob Agents Chemother 57: 1082–1085.
15. Silverman JA, Perlmutter NG, Shapiro HM (2003) Correlation of daptomycin bactericidal activity and membrane depolarization in *Staphylococcus aureus*. Antimicrob Agents Chemother 47: 2538–2544.
16. Tran TT, Panesso D, Mishra NN, Mileykovskaya E, Guan Z, et al. (2013) Daptomycin-resistant *Enterococcus faecalis* diverts the antibiotic molecule from the division septum and remodels cell membrane phospholipids. mBio 4.
17. Yang SJ, Kreiswirth BN, Sakoulas G, Yeaman MR, Xiong YQ, et al. (2009) Enhanced expression of *dltABCD* is associated with development of daptomycin nonsusceptibility in a clinical endocarditis isolate of *Staphylococcus aureus*. J Infect Dis 200: 1916–1920.
18. Yang S-J, Nast CC, Mishra NN, Yeaman MR, Fey PD, et al. (2010) Cell wall thickening is not a universal accompaniment of the daptomycin nonsusceptibility phenotype in *Staphylococcus aureus*: evidence for multiple resistance mechanisms. Antimicrob Agents Chemother 54: 3079–3085.
19. Bayer AS, Schneider T, Sahl H-G (2013) Mechanisms of daptomycin resistance in *Staphylococcus aureus*: role of the cell membrane and cell wall. Ann N Y Acad Sci 1277: 139–158.
20. Humphries RM, Pollett S, Sakoulas G (2013) A current perspective on daptomycin for the clinical microbiologist. Clin Microbiol Rev 26: 759–780.
21. Kaatz GW, Lundstrom TS, Seo SM (2006) Mechanisms of daptomycin resistance in *Staphylococcus aureus*. Int J Antimicrob Agents 28: 280–287.
22. Ganz T, Selsted ME, Lehrer RI (1990) Defensins. Eur J Haematol 44: 1–8.
23. Yeaman MR, Yount NY (2003) Mechanisms of antimicrobial peptide action and resistance. Pharmacol Rev 55: 27–55.
24. Yang SJ, Xiong YQ, Dunman PM, Schrenzel J, Francois P, et al. (2009) Regulation of *mprF* in daptomycin-nonsusceptible *Staphylococcus aureus*. Antimicrob Agents Chemother 53: 2636–2637.
25. Mishra NN, McKinnell J, Yeaman MR, Rubio A, Nast CC, et al. (2011) *In vitro* cross-resistance to daptomycin and host defense cationic antimicrobial peptides in clinical methicillin-resistant Staphylococcus aureus isolates. Antimicrob Agents Chemother 55: 4012–4018.
26. Mishra NN, Yang SJ, Sawa A, Rubio A, Nast CC, et al. (2009) Analysis of cell membrane characteristics of *in vitro*-selected daptomycin-resistant strains of methicillin-resistant *Staphylococcus aureus* (MRSA). Antimicrob Agents Chemother 53: 2312–2318.
27. Mishra NN, Liu GY, Yeaman MR, Nast CC, Proctor RA, et al. (2011) Carotenoid-related alteration of cell membrane fluidity impacts *Staphylococcus aureus* susceptibility to host defense peptides. Antimicrob Agents Chemother 55: 526–531.
28. Bertsche U, Yang S-J, Kuehner D, Wanner S, Mishra NN, et al. (2013) Increased cell wall teichoic acid production and D-alanylation are common phenotypes among daptomycin-resistant methicillin-resistant *Staphylococcus aureus* (MRSA) clinical isolates. PLoS ONE 8: e67398.
29. Bertsche U, Weidenmaier C, Kuehner D, Yang S-J, Baur S, et al. (2011) Correlation of daptomycin resistance in a clinical *Staphylococcus aureus* strain with increased cell wall teichoic acid production and D-alanylation. Antimicrob Agents Chemother 55: 3922–3928.
30. Baba T, Takeuchi F, Kuroda M, Yuzawa H, Aoki K-i, et al. (2002) Genome and virulence determinants of high virulence community-acquired MRSA. The Lancet 359: 1819–1827.
31. Cafiso V, Bertuccio T, Purrello S, Campanile F, Mammina C, et al. (2014) *dltA* overexpression: A strain-independent keystone of daptomycin resistance in methicillin-resistant *Staphylococcus aureus*. Int J Antimicrob Agents 43: 26–31.
32. Ernst C, Staubitz P, Mishra NN, Yang SJ, Hornig G, et al. (2009) The bacterial defensin resistance protein MprF consists of separable domains for lipid lysinylation and antimicrobial peptide repulsion. PLos Pathogens 5.
33. Weidenmaier C, Peschel A, Kempf VAJ, Lucindo N, Yeaman MR, et al. (2005) DltABCD- and MprF-mediated cell envelope modifications of *Staphylococcus aureus* confer resistance to platelet microbicidal proteins and contribute to virulence in a rabbit endocarditis model. Infect Immun 73: 8033–8038.
34. Yang S-J, Mishra NN, Rubio A, Bayer AS (2013) Causal role of single nucleotide polymorphisms within the mprF gene of Staphylococcus aureus in daptomycin resistance. Antimicrob Agents Chemother 57: 5658–5664.
35. Mishra NN, Yang S-J, Chen L, Muller C, Saleh-Mghir A, et al. (2013) Emergence of daptomycin resistance in daptomycin-naïve rabbits with methicillin-resistant Staphylococcus aureus prosthetic joint infection is associated with resistance to host defense cationic peptides and mprF polymorphisms. PLoS One 8: e71151.
36. Clinical and Laboratory Standards Institute (2012) Performance standards for antimicrobial susceptibility testing; 20th informational supplement, M100-S22. CLSI, Wayne, PA.
37. Yang S-J, Bayer AS, Mishra NN, Meehl M, Ledala N, et al. (2012) The *Staphylococcus aureus* two-component regulatory system, GraRS, senses and confers resistance to selected cationic antimicrobial peptides. Infect Immun 80: 74–81.
38. Keynan Y, Rubinstein E (2013) *Staphylococcus aureus* bacteremia, risk factors, complications, and management. Critical Care Clinics 29: 547–562.
39. Peschel A, Otto M, Jack RW, Kalbacher H, Jung G, et al. (1999) Inactivation of the dlt operon in Staphylococcus aureus confers sensitivity to defensins, protegrins, and other antimicrobial peptides. J Biol Chem 274: 8405–8410.
40. Weidenmaier C, Kokai-Kun JF, Kristian SA, Chanturiya T, Kalbacher H, et al. (2004) Role of teichoic acids in Staphylococcus aureus nasal colonization, a major risk factor in nosocomial infections. Nat Med 10: 243–245.
41. Kristian SA, Datta V, Weidenmaier C, Kansal R, Fedtke I, et al. (2005) D-alanylation of teichoic acids promotes group a streptococcus antimicrobial peptide resistance, neutrophil survival, and epithelial cell invasion. J Bacteriol 187: 6719–6725.
42. Cui L, Tominaga E, Neoh H-m, Hiramatsu K (2006) Correlation between reduced daptomycin susceptibility and vancomycin resistance in vancomycin-intermediate *Staphylococcus aureus*. Antimicrob Agents Chemother 50: 1079–1082.
43. Yeaman MR, Puentes SM, Norman DC, Bayer AS (1992) Partial characterization and staphylocidal activity of thrombin-induced platelet microbicidal protein. Infect Immun 60: 1202–1209.
44. Sieprawska-Lupa M, Mydel P, Krawczyk K, Wojcik K, Puklo M, et al. (2004) Degradation of human antimicrobial peptide LL-37 by *Staphylococcus aureus*-derived proteinases. Antimicrob Agents Chemother 48: 4673–4679.
45. Yeaman MR, Bayer AS, Koo S-P, Foss W, Sullam PM (1998) Platelet microbicidal proteins and neutrophil defensin disrupt the *Staphylococcus aureus* cytoplasmic membrane by distinct mechanisms of action. J Clin Invest 101: 178–187.
46. Yeaman MR, Gank KD, Bayer AS, Brass EP (2002) Synthetic peptides that exert antimicrobial activities in whole blood and blood-derived matrices. Antimicrob Agents Chemother 46: 3883–3891.
47. Dyer DW, Iandolo JJ (1983) Rapid isolation of DNA from *Staphylococcus aureus*. Appl Environ Microbiol 46: 283–285.
48. Yang S-J, Xiong YQ, Yeaman MR, Bayles KW, Abdelhady W, et al. (2013) Role of the LytSR two-component regulatory system in adaptation to cationic antimicrobial peptides in *Staphylococcus aureus*. Antimicrob Agents Chemother 57: 3875–3882.
49. Kilelee E, Pokorny A, Yeaman MR, Bayer AS (2010) Lysyl-phosphatidylglycerol attenuates membrane perturbation rather than surface association of the cationic antimicrobial peptide 6W-RP-1 in a model membrane system: implications for daptomycin resistance. Antimicrob Agents Chemother 54: 4476–4479.
50. Pillai SK, Gold HS, Sakoulas G, Wennersten C, Moellering RC Jr, et al. (2007) Daptomycin nonsusceptibility in *Staphylococcus aureus* with reduced vancomycin susceptibility is independent of alterations in MprF. Antimicrob Agents Chemother 51: 2223–2225.
51. Center for Disease Control and Prevention (1999) Four pediatric deaths from community-acquired methicillin-resistant *Staphylococcus aureus*-Minnesota and North Dakota,1997–1999. Morb Wkly Rep 48: 707–710.
52. Mishra NN, Bayer AS, Moise PA, Yeaman MR, Sakoulas G (2012) Reduced susceptibility to host-defense cationic peptides and daptomycin coemerge in methicillin-resistant *Staphylococcus aureus* from daptomycin-naive bacteremic patients. J Infect Dis 206: 1160–1167.
53. Mishra NN, Bayer AS, Tran TT, Shamoo Y, Mileykovskaya E, et al. (2012) Daptomycin resistance in enterococci Is associated with distinct alterations of cell membrane phospholipid content. PLoS ONE 7: e43958.
54. Beranová J, Jemioła-Rzemińska M, Elhottová D, Strzałka K, Konopásek I (2008) Metabolic control of the membrane fluidity in *Bacillus subtilis* during cold adaptation. Biochim Biophys Acta 1778: 445–453.